Treatment of two sartan antihypertensives in water by photo-electro-Fenton using BDD anodes: Comparative degradation, theoretical analyses, primary transformations and matrix effects

Diana Martínez-Pachón[a], Efraím A Serna-Galvis[b], María Ibañez[c], Félix Hernández[c], Yenny Ávila-Torres[d], Ricardo A. Torres-Palma[b,*], Alejandro Moncayo-Lasso[a,*]

[a]Grupo de Investigación en Ciencias Biológicas y Químicas, Facultad de Ciencias, Universidad Antonio Nariño (UAN), Bogotá D.C., Colombia.

[b]Grupo de Investigación en Remediación Ambiental y Biocatálisis (GIRAB), Instituto de Química, Facultad de Ciencias Exactas y Naturales, Universidad de Antioquia UdeA, Calle 70 No. 52-21, Medellín, Colombia.

[c]Research Institute for Pesticides and Water (IUPA), University Jaume I (UJI), Castellón, Spain.

[d]Grupo de Investigación QUIBIO, Facultad de Ciencias Básicas, Universidad Santiago de Cali, Santiago de Cali, Pampalinda, Colombia.

***Correspondence:**

amoncayo@uan.edu.co (Alejandro Moncayo-Lasso)

ricardo.torres@udea.edu.co (Ricardo A. Torres-Palma)

Abstract

Degradation of two representative antihypertensives, losartan (LOS) and valsartan (VAL), in water by photo-electro-Fenton (PEF) using a BDD anode and a gas diffusion cathode in presence of sulfate anion was evaluated. Initially, ability of anodic oxidation, electro-peroxidation, and PEF to degrade LOS and VAL was tested. PEF showed the highest elimination (>95% at 30 and 60 min of treatment for LOS and VAL, respectively). The degradation rate constants were 0.154 and 0.054 min^{-1} for LOS and VAL, correspondently. Theoretical analyses of atomic charges were then performed to rationalize the antihypertensives reactivity toward the electrogenerated oxidizing agents. Afterwards, the primary transformations induced by PEF to the pollutants were assessed. The products revealed that the electrogenerated oxidizing species attack the biphenyl-tetrazole, imidazole, and alcohol moieties on LOS. Meanwhile, carboxylic and amide groups, plus the central nucleus, were modified on VAL. These moieties corresponded well with the electron-rich sites indicated by the theoretical calculations. On the other hand, the PEF process removed between 33 and 38% of total organic carbon after 5h of electrolysis. Finally, it was considered the LOS treatment in the presence of oxalic acid (a typical organic waste of pharmaceutical industry), in addition to the pollutant degradation in effluents of municipal sewage treatment plant by PEF at a pH close to five. Oxalic acid accelerated LOS degradation. Meanwhile, in the effluent, the process led to 64% of LOS removal after 120 min of treatment, indicating the high potentiality of PEF to degrade LOS in water containing organic and inorganic substances.

Keywords: Advanced oxidation process; Electrochemical techniques; Losartan; Pollutant elimination; Valsartan; Water treatment.

1 Introduction

Sartan-type antihypertensives are highly prescribed pharmaceuticals, which, after consumption, are partially metabolized, and thus significant amounts are excreted into the sewage system (Israili, 2000). Indeed, these sartan-type antihypertensives are frequently found in influents of municipal wastewater treatment plants (Botero-Coy et al., 2018; Gurke et al., 2015; Kaur and Dulova, 2020). Furthermore, the conventional processes (as secondary biological systems) cannot completely degrade sartan-type antihypertensives. Consequently, unmodified or partially modified antihypertensives are released into the environment through municipal wastewater treatment plants (Botero-Coy et al., 2018; Gurke et al., 2015; Kaur and Dulova, 2020). It must be mentioned that LOS and VAL are among the most prescribed/consumed antihypertensives worldwide. For instance, ~52 and ~9 million of losartan and valsartan prescriptions were done in the USA during 2017 (ClinClac, 2018; Mikulic, 2020). Additionally, it is reported that in the environment, sartan-type antihypertensives as losartan (LOS) or valsartan (VAL) are transformed into valsartan-acid, which is a persistent substance (Berkner and Thierbach, 2014; Nödler et al., 2013). Hence, processes to efficiently degrade sartan-type pollutants in aqueous matrices and limit their input to natural media are required.

Among processes that have shown high efficiency for degrading toxic and/or recalcitrant pollutants are electrochemical treatments (Dao et al., 2020; Moreira et al.,

2017). Particularly, the electrochemical treatments involving the utilization of hydroxyl radical (HO•, E°: 2.8 V) possess a high ability to transform the organic pollutants into innocuous substances (even up to mineralization) (Feng et al., 2019; Moreira et al., 2017). Electrochemical processes have high cost-effectiveness in electric energy consumption, versatility, and environmental compatibility (Salazar et al., 2016).

In this work is studied the electrochemical treatment, mainly PEF using BDD anodes, of LOS and VAL. Degradation under mild electrochemical conditions (low current density, low UVA power, and small iron concentration) was tested. Although previous researches have tested the degradation of LOS using electro-oxidation (Salazar et al., 2016), such work does not present the pollutant's treatment in complex water matrices as effluents of municipal wastewater treatment plants.

Also, it must be mentioned that LOS and VAL eliminations by PEF using DSA anodes and sodium chloride as supporting electrolytes have been informed (Martínez-Pachón et al., 2019, 2018). However, this configuration involves active chlorine action, which may lead to the formation of concern organochlorinated compounds. Moreover, under the authors' knowledge, the utilization of theoretical calculations (to study the antihypertensives reactivity) has not been reported. Thus, herein, it was considered the treatment of both antihypertensives by electrochemical processes based on BDD as anode and sodium sulfate as supporting electrolyte (to promote the action of radicals more than chlorine species). Furthermore, atomic charge analyses were performed to study the pollutants reactivity toward oxidizing agents generated in the electrochemical processes.

Therefore, our work develops four main topics: 1) Evaluation of the efficiency of anodic oxidation, electro-peroxidation and photo-electro-Fenton (PEF) processes to degrade LOS and VAL individually; 2) Testing of the antihypertensive structure effect on the elimination by PEF, comparing the elimination of losartan and valsartan, and performing theoretical analyses of atomic charge to provide a basic idea about the reactivity of the antihypertensives toward oxidizing agents; 3) Determination of primary transformation products (by using HPLC-MS technique) and mineralization of both antihypertensives by PEF action; 4) Assessment of matrix effects through degradation of the LOS in effluents of municipal wastewater treatment plant by PEF at a pH higher than 3.0, in addition to the treatment in the presence of a typical organic waste of pharmaceutical industry.

2 Materials and Methods

2.1 Reagents

Valsartan and losartan potassium (99% purity) were purchased from Sigma Aldrich. Iron (II) sulfate heptahydrate ($FeSO_4.7H_2O$), potassium phosphate dibasic (K_2HPO_4), orthophosphoric acid (H_3PO_4), potassium hydrogen phthalate ($C_8H_5KO_4$), oxalic acid ($C_2H_2O_4$) and sodium sulfate (Na_2SO_4) were analytical grade from Merck. The pH of the solutions was adjusted using chlorhydric acid (HCl, 98% purity). Methanol (MeOH) and acetonitrile (CH_3CN) HPLC-grade were obtained from Panreac. All solutions were prepared with ultrapure water produced by a Millipore Milli-Q system with resistivity > 18 MΩ cm at 25 °C, and the experiments were carried out at least by duplicate. For UHPLC-HRMS analysis, HPLC-grade water was obtained by purifying demineralized water using a Milli-Q system from Millipore (Bedford, MA, USA). HPLC-grade methanol

and acetonitrile, formic acid, acetone, and sodium hydroxide were acquired from Scharlau. Leucine enkephalin was purchased from Sigma-Aldrich (St. Louis, MO, USA).

2.2. Reaction systems

For the anodic oxidation (AO) and electro-peroxidation (EP), the electrode arrangements were boron-doped diamond anode/stainless steel cathode; and graphite anode/gas diffusion cathode, respectively. The degradation experiments were carried out in an open undivided 250-mL electrolytic cell, operated in batch mode at room temperature. A carbon-felt air diffusion cathode (GDE, 2 cm^2), a stainless-steel cathode (SS, 2 cm^2), a boron-doped diamond anode (BDD, 2.0 cm^2), and a graphite cathode (2 cm^2) were used. The electrodes were located in the center of the reactor at 2.0 cm of distance, and the system was operated at constant current mode (5.0 mA/cm^2). The electrochemical cell, containing LOS or VAL that were individually treated (200 mL, at 45 μmol/L each) was bubbled with air obtained from an air compressor to saturate the solution with oxygen and continuously stirred (400 rpm on a magnetic stirrer ARECT by VELP Scientifica). Sodium sulfate (0.05 mol/L) was used as supporting electrolyte, and when was necessary, the initial pH-value was adjusted with hydrochloric acid solution (0.1 mol/L). For photo-electro-Fenton (PEF, which used BDD and GDE) process, Fe^{2+} ions (36 μmol/L) were added to the solution, and it was irradiated with a UVA light lamp (fluorescent black-light blue tube Toshiba FL4BLB/4 W, wavelength 368 nm, photoionization energy input of 1.4 W/m^2) placed inside the cell. Some experiments were carried out to evaluate the LOS degradation by PEF at higher pH values and in aqueous matrices more complex than distilled water. In such

case, the PEF process was carried out in the presence of oxalic acid (40 µmol/L) without pH modification and doping with LOS the effluent of the wastewater treatment plant Salitre-Bogotá-Colombia (EWWTP).

2.3 Analyses

The antihypertensives degradation was followed using an HPLC Shimadzu LC-20AT equipped with a photodiode array detector SPD-M20A and a C18 column (Waters Spherisil ODS 2, 250 mm × 4.6 mm i.d., 5 µm particle size). The mobile phase was composed of phosphate buffer (pH 3.5, 0.01 mol/L)/ acetonitrile/ methanol (44/46/10 v/v/v) at 25 °C, using isocratic conditions). The mixture was pumped at 1.0 mL/min flow rate, and the detector was set up at 254 nm. Under these conditions, LOS and VAL were eluted at 3.5 min and 6.9 min, respectively.

Transformation products were elucidated by UHPLC-HRMS, using a Waters Acquity UHPLC system (Waters, Milford, MA, USA), coupled to a hybrid quadrupole-orthogonal acceleration-time of flight mass spectrometer (XEVO G2 QTOF, Waters Micromass, Manchester, UK), with an orthogonal Z-spray-ESI interface, operated in both positive and negative ionization modes. Additional details on instrumental conditions can be seen elsewhere (Martínez-Pachón et al. 2019; Serna-Galvis et al. 2019).

For MS^E experiments, two functions were acquired: for the low energy function (LE) collision energy of 4 eV was selected whereas for the high energy (HE) function, a collision energy ramp from 15 to 40 eV was applied, in order to obtain a greater range of fragment ions. Additional MS/MS experiments at different collision energies (10, 20,

30, 40 and 50 eV) were also performed. Mass data were acquired with MassLynx v 4.1 (Waters).

Accumulation of hydrogen peroxide electrogenerated was estimated by iodometry (Serna-Galvis et al., 2015). An aliquot of 30 µL from the reactor was added to a quartz cell containing 1920 µL of potassium iodide (0.1 mol/L) and 50 µL of ammonium heptamolybdate (0.01 mol/L). The sample was homogenized using a vortex mixer, and after 5 min, the absorbance at 350 nm was measured using a Mettler Toledo UV5 spectrophotometer.

The mineralization of LOS and VAL treated solutions were monitored by the abatement of total organic carbon (TOC), which was measured using a Shimadzu LCSH TOC analyzer. The TOC was determined by combustion with catalytic oxidation at 680 °C using high-purity oxygen as the carrying gas at a flow rate of 190 mL/min with a non-dispersive infrared detector. The calibration of the analyzer was attained with standard potassium hydrogen phthalate (99.5%) solution.

Theoretical analyses of atomic charge (AC, which provides a basic idea on the electron density (Ionescu et al., 2015)) for losartan and valsartan were performed by using the free online AtomicChargeCalculator© (version 1.0.17.1.26) software by loading the structure of the molecules in PDB or SDF format (Sehnal, 2020).

3. Results and Discussion

3.1 Antihypertensives degradation by three electrochemical systems

Initially, the degrading ability of anodic oxidation (AO), electro-peroxidation (EP), and photo-electro-Fenton (PEF) were tested. Fig. 1A presents the evolution of both

178 pollutants under these processes. It can be noted that the degradations of VAL and
179 LOS for AO and EP systems were 13-17% and 50-56% after 60 min of treatment,
180 respectively. Meanwhile, at 30 min of electrolysis, PEF achieved ~ 80 and 100% of the
181 VAL and LOS removals. The pollutants elimination in the AO may involve the action of
182 hydroxyl radical physisorbed on the BDD anode and the persulfate electrogenerated
183 from the supporting electrolyte (i.e., the mediated routes, Eq. 1-3), in addition to direct
184 oxidation by electron transfer from the pharmaceuticals to the anode (Eq. 4) (Davis et
185 al., 2014; Salazar et al., 2016). Such degradation routes depend on the diffusion of the
186 pollutant or sulfate electrolyte toward the electrode surface and the current density
187 (Sirés and Brillas, 2012). As under tested conditions, the current density is low (which
188 is 5.0 mA/cm^2), the production of radicals or persulfate is low (as supported by the very
189 low accumulation of oxidizing species for AO, Fig. S1 in the Supporting information)
190 and the direct oxidation of the pollutants is limited (Sirés and Brillas, 2012). Thereby,
191 the degradation extent of LOS or VAL by AO is also limited (lower than 20% in 1 h)
192 (Fig. 1A).

$$BDD\ (HO^{\bullet}) + LOS/VAL \rightarrow \text{degradation products} \quad (1)$$

$$BDD + 2SO_4^{2-} \rightarrow S_2O_8^{2-} + 2e^- \quad (2)$$

$$S_2O_8^{2-} + LOS/VAL \rightarrow \text{degradation products} \quad (3)$$

$$BDD + LOS/VAL \rightarrow \text{degradation products} + ne^- \quad (4)$$

193 In the case of the EP system, although graphite anode cannot generate physisorbed
194 radicals as BDD, direct oxidation of organic pollutants as LOS or VAL can occur by
195 electron transfer to the anode or interaction with oxygen on the graphite surface (Eq.
196 5-7) (Rueffer et al., 2011). Additionally, in the considered EP configuration, H_2O_2 is

197 electrogenerated from the oxygen reduction in the GDE (Eq. 8) (indeed, the H_2O_2
198 accumulation for the EP is evidenced in Fig. SM1). Hydrogen peroxide is an oxidizing
199 agent that may also contribute to the removal of the antihypertensives (Eq. 8-9) (Sirés
200 et al., 2014). Then, the simultaneous action of anodic routes plus the electrogenerated
201 hydrogen peroxide makes the EP more efficient than AO for the elimination of LOS
202 and VAL (Fig. 1A).

$$C_{graphite} + LOS/VAL \rightarrow \text{degradation products} + ne- \quad (5)$$

$$C_{graphite} + 2H_2O \rightarrow C\text{-}O\text{-}OH + 2H^+ + 2e- \quad (6)$$

$$C\text{-}O\text{-}OH + LOS/VAL \rightarrow C\text{-}OH + \text{degradation products} \quad (7)$$

$$GDE + O_2 + 2H^+ + 2e- \rightarrow H_2O_2 \quad (8)$$

$$H_2O_2 + LOS/VAL \rightarrow \text{degradation products} \quad (9)$$

203 In the PEF system, which is formed by the BDD anode, the GDE cathode plus UVA
204 light, and iron, present the action of radicals (hydroxyl and sulfate radicals, Eqs.10-13),
205 in addition to the degrading routes of anodic oxidation and reaction with H_2O_2.
206 Photolysis of both antihypertensives by the light was discarded because UVA
207 irradiation showed no significant pollutant elimination even after 60 min of treatment
208 (Fig. SM2). This can be explained considering that there is no intersection between the
209 lamp emission (which is a peak centered at 368 nm) and the UV spectra of LOS and
210 VAL (These have absorptions at wavelengths <340 nm (Bonfilio et al., 2010; Singh et
211 al., 2011)). The important UVA role is evidenced when the photo-electro-Fenton
212 process is faced with its control, the electro-Fenton system (EF).

213 Fig. 1B compares LOS degradation by EF and PEF, which had removals of 41 and
214 58% in the first 5 min of treatment, respectively. Likewise, Fig. 1C shows the

elimination of VAL by EF and PEF, where PEF also exerted a higher removal of the pollutant. The elimination of the antihypertensives is increased in PEF respect to EF thanks to the regeneration of the ferrous ions is accelerated by the UVA light, which subsequently raises the number of radicals (HO• and $SO_4^{\bullet -}$) available (Eqs. 10-13) to degrade LOS or VAL. Hence, it can be indicated that the PEF system combines the routes of anodic oxidation, reactions with the electrogenerated H_2O_2 plus a strong action of radicals coming from the interaction among iron, H_2O_2 or $S_2O_8^{2-}$ and UVA light (which is supported by the relative high oxidant accumulations during the treatments of LOS or VAL by PEF, see Fig. SM3). Consequently, this leads to a higher degradation of the pollutants by PEF than by AO, EP, or EF system (Fig. 1A-C). Thus, due to the best performance of PEF for degrading LOS (mainly associated with the action of radicals), such system is utilized for the subsequent experiments.

Figure 1

$$Fe^{2+} + H_2O_2 \rightarrow Fe^{3+} + HO\bullet + HO^- \quad (10)$$

$$Fe^{2+} + S_2O_8^{2-} \rightarrow Fe^{3+} + SO_4^{\bullet -} + SO_4^{2-} \quad (11)$$

$$HO\bullet, SO_4^{\bullet -} + \text{LOS/VAL} \rightarrow \text{degradation products} \quad (12)$$

$$Fe^{3+} + H_2O + UVA \rightarrow Fe^{2+} + HO\bullet + H^+ \quad (13)$$

3.2 Effect of the antihypertensive structure - Losartan vs. Valsartan

LOS and VAL belong to sartan-type antihypertensives, which comprises several compounds sharing a common nucleus. Indeed, LOS was the first antihypertensives-type, and the synthesis of the other sartans was based on its structure (Nödler et al., 2013). The pharmaceuticals LOS and VAL contain a biphenyl-tetrazole nucleus; LOS

additionally has chlorine, butyl, and methoxy groups bonded to an imidazole ring, whereas VAL exhibits a carboxylic acidic linked to a pentanamide moiety (Tables SM1-SM2).

Figure 2

As observed from Fig. 1, LOS exhibited a faster degradation than VAL, especially in the PEF system. To better understand the differences, kinetics and structural aspects were considered. The degradations of VAL and LOS by PEF adjusted well to pseudo-first-order kinetics (i.e., the plots of Ln (C/Co) vs. time of these antihypertensives have a linear form, Fig. 2). The corresponding degradation rate constants (k) for LOS and VAL were 0.154 and 0.054 min^{-1}, respectively. The unlike k values could be related to differences in LOS and VAL interaction with the degrading agents.

The degrading species involved in the PEF process (i.e., hydrogen peroxide, persulfate anion or radicals, even the anode) typically attack the regions rich in electron density on the pollutants (Serna-Galvis et al. 2017). Hence, theoretical analyses of atomic charge (AC) for LOS and VAL were performed (Tables SM1-SM2) to provide a rough idea of electron density on the antihypertensives (Ionescu et al., 2015)). A more negative value of AC indicates a higher electron density. From Tables SM1-SM2, it can be noted that the antihypertensives have different atomic charge distributions, even in the common nucleus that they differ. In fact, the addition of charges corresponding to tetrazole moiety is more negative for LOS than for VAL. Furthermore, the charges summation of all substituents attached at the common nucleus for LOS (Σ = -0.040 -0.359 -0.068 +0.391 = -0.076) is more negative than for VAL (Σ = -0.420 +0.620 -0.213 = -0.013), which suggests that globally the substituents on LOS have more electron

density than those on VAL. Consequently, LOS exhibits a higher reactivity toward the degrading species (i.e., this antihypertensive is easier to oxidize), which explains its faster degradation (and a higher k value) by the PEF system (Fig. 2).

3.3 Primary transformations of the antihypertensives and mineralization by PEF action

To deeply study the PEF action on the target pollutants, the initial transformations were established through UHPLC-HRMS analyses. Table SM3 presents the chemical structure of the primary degradation products of losartan (DPL). Three products coming from imidazole ring rupture (DPL1, DPL2, and DPL3), several isomers of hydroxylation of the biphenyl-tetrazole moiety (DPL4-10) and one product of alcohol group oxidation (DPL11) were found. In the case of VAL, products generated after decarboxylation (DPV1), hydroxylations of tetrazole (DPV2), biphenyl (generating three isomers, DPL3-6) and amide (DPV7), in addition to oxidation (DPV8) the linear-alkyl group on the pentanamide moiety were identified (Table SM4). MS/MS information about these TPs can be found in a recent paper (Serna-Galvis et al., 2019), where these two hypertensives were subjected to sonochemical degradation.

In addition to the structural elucidation, the normalized evolution of the products was established (Figs. SM4-SM5). It can be observed that DPL1, DPL2, DPL3, and DPL11 are faster formed than the other products. This indicates that imidazole and alcohol on LOS are the most reactive sites to the degrading agents. Indeed, radical species (as HO•) fastly interacts with heterocyclic rings as imidazoles (Llano and Eriksson, 1999), because such functional groups have a high electron availability (as indicated by the theoretical analyses of atomic charges presented in Table SM1). The successive

attacks of radical species can promote the imidazole ring-opening (Cheng et al., 2010), as observed from the structure of DPL1, DPL2, and DPL3.

Furthermore, it can be mentioned that alcohols are also prone to oxidation by radicals through hydrogen abstraction to produce the respective aldehyde. Indeed, alcohols are typically used as scavengers due to their high reactivity towards hydroxyl or sulfate radicals (Billany et al., 1996; He et al., 2014). This explains the favorable attack by the radicals to the alcohol group on LOS to generate DPL11.

The high number of isomers by attacks to the biphenyl-tetrazole nucleus (DPL 4-10) suggests that such a portion of LOS is also very reactive towards electron-deficient degrading species. It is recognized that HO• and $SO_4^{\bullet -}$ can react with double bonds on the benzene rings (which also concentrate electron density, as reflected by the negative charges on carbons of the biphenyl moiety in Table SM1), to produce hydroxylated substances (He et al., 2014; Khan et al., 2017; Liu et al., 2016). In turn, the tetrazole group (another electron-rich region on LOS, see Table SM1) is also susceptible to hydroxylation by the action of the radicals. It has been proposed that the successive attacks of radical species to such moiety can also cleavage this ring (Gurkan et al., 2012).

Regarding transformation products from VAL, it can be noted that DPV1 and DPV2 are firstly formed (Fig. SM5), indicating the high reactivity of tetrazole and carboxylic acid moieties on the antihypertensive. This was also coincident with the most negative values obtained for these moieties from the atomic charge analyses for VAL (Table SM2). As previously mentioned, the tetrazole group can experiment hydroxylations by the radicals' action, and it is well-known that HO• and $SO_4^{\bullet -}$ can promote decarboxylations of organic molecules (Steffen et al., 1991; Yang et al., 2015). Similar

303 to LOS, some isomers from hydroxylations to the biphenyl group are formed (Table
304 SM4), due to this molecular region on VAL has a considerable electron density (see
305 the negative charges on carbons of such moiety in Table SM2). Additionally, it can be
306 noted that the pentanamide group of VAL also concentrates electron density, which
307 makes this part of the pollutant very available for attacks of the electron-deficient
308 degrading species, leading to DPV7 and DPV8 formation.
309 Interestingly, the degradations of LOS by other electrochemical, sonochemical and
310 photochemical (based on UVC) processes have also reported products formed through
311 attacks of the radical species to biphenyl-tetrazole rings, imidazole and alcohol
312 moieties (Kaur and Dulova 2020; Martínez-Pachón et al. 2018, 2019; Salazar et al.
313 2016; Serna-Galvis et al. 2019). Likewise, in VAL, strong modifications to the
314 carboxylic and amide groups have also been found by other electrochemical systems
315 (Martínez-Pachón et al., 2019). Moreover, during the sonochemical treatment of
316 antihypertensive, same DPV2, DVP7, and DPV8 were obtained (Serna-Galvis et al.
317 2019) than in our treatment by PEF. The similarities between the degradation products
318 obtained by PEF and those reported for other processes in the literature suggest
319 identical elimination routes, which is logical, considering that the main degrading role
320 is exerted by the radicals such as HO• and $SO_4^{\bullet -}$.
321 It is important to remark that the primary transformations induced by the PEF process
322 and reported in the literature agree well the reactive sites on LOS and VAL indicated
323 by the theoretical analyses presented in the previous section (Tables SM1-SM2). This
324 reveals the high utility of atomic charge analyses as a qualitative-predictive tool for
325 understanding the initial transformations induced by processes as PEF.

After understanding the primary transformations of both LOS and VAL by PEF, the mineralization of these pollutants was tested. Fig. 3 shows the TOC evolution. As seen, the TOC decreasing is fast until the first 60 min of treatment, reaching ~ 18% of mineralization. Nevertheless, TOC elimination is slowly increased to 33-38%% after 5h of electrolysis. This suggests that the compounds coming from the primary products of LOS or VAL degradations are more recalcitrant to the action of the PEF process (Martínez-Pachón et al., 2018).

As evidenced by the chemical structures of the primary products (Tables SM3-SM4), the PEF process's first transformations lead to oxidations, hydroxylations, fragmentations (even decarboxylation) of the parent pollutants. It is well-known that the subsequent steps generate short-chain molecules (e.g., aliphatic acids) from the primary intermediates by the treatment action. Such short-chain molecules are recalcitrant to the action of radicals as HO• and trend to accumulate in the solution (Antonin et al., 2015; Skoumal et al., 2009), as also reported for treatment of VAL by PEF using DSA anodes (which exhibited the accumulation of succinic and malic acids after 5h of the electrochemical process application) (Martínez-Pachón et al., 2018). It can be mentioned that highly oxidized, and short-chain molecules (e.g., aliphatic acids) are biocompatible (Feng et al., 2019; Martínez-Pachón et al., 2018). then, it can be suggested that this electrochemical system may transform both LOS and VAL into products more friendly for the environment.

Figure 3

3.4 Matrix effect on the LOS degradation by PEF

In the previous sections, it has been considered the degradation of the antihypertensives in the simplest matrix (distilled water) and at the ideal pH for the Fenton-based processes (i.e., pH ~ 3.0, (Antonin et al., 2015; Pignatello et al., 2006)). However, the actual applications of the PEF process demand the operation at higher pH values and in aqueous matrices more complex than distilled water. Therefore, in this research, we tested the degradation of LOS (which was selected because its fastest degradation in the simplest matrix, Fig. 1A) by PEF at pH 5.0 and in the presence of oxalic acid (an organic compound widely used at the pharmaceutical manufacture (Transparency Market Research, 2020), which can be present in wastewaters of such industries). Also, the treatment by PEF of a real effluent of municipal wastewater treatment plant doped with LOS was performed. These topics are detailed below.

In Fig. 4A, the removal of LOS by PEF at pH 3.0 and pH 5.0 is compared. It can be noted that although at pH 5.0, the degradation was slower than at pH 3.0, the process completely degraded the antihypertensive after 90 min of treatment. The differences at each pH can be associated with iron's aqueous chemistry, mainly the speciation of Fe (III). Despite at pH 5.0, the first step of Fenton reaction involves a species (i.e., $[Fe(H_2O)_4(OH)_2]$, Eq. 14) ~ 10 times more reactive than Fe^{2+} (which predominates at pH 3.0, Eqs. 10-11) toward hydrogen peroxide, at the less acidic pH, a portion of the Fe (III) ions experiments precipitation as amorphous ferric oxyhydroxides (Eq. 15). These oxyhydroxides are little photo-active, and due to their colloidal nature, they may scatter the light (Pignatello et al., 2006). This limits the production of radicals through Eq. 13. Consequently, this decreases the rate of pollutant degradation (as observed for LOS in Fig. 4A).

$$[Fe(H_2O)_4(OH)_2] + H_2O_2 \rightarrow [Fe(H_2O)_4(OH)_2]^+ + HO\bullet + HO^- \quad (14)$$

$$[Fe(H_2O)_4(OH)_2]^+ + HO^- \rightarrow\rightarrow\rightarrow \text{other polynuclear species} \quad (15)$$

Interestingly, in the presence of oxalic acid at pH 5.4, the LOS removal was improved respect to degradation at pH 5.0, achieving 100% of pollutant elimination after 45 min of the process application (Fig. 4A). The oxalic acid is a well-known complexing agent of Fe (III) (Eq. 16), and its presence in the aqueous media avoids the precipitation of iron as ferric oxyhydroxides (Martínez-Pachón et al., 2018; Pignatello et al., 2006). The ferric-oxalic acid complexes are soluble forms susceptible to photo-decomposition by UVA light action through a ligand to metal charge transfer mechanism (Eq. 17) (Martínez-Pachón et al., 2018; Pignatello et al., 2006), explaining the positive effect of the presence of oxalic acid at pH 5.4. Hence, these results suggest that PEF can effectively treat pharmaceutical wastewater, having mixtures of oxalic acid and LOS.

$$Fe^{3+} + 3C_2O_4^{2-} \rightarrow [Fe(C_2O_4)_3]^{3-} \quad (16)$$

$$2[Fe(C_2O_4)_3]^{3-} + UVA \rightarrow 2Fe^{2+} + 4C_2O_4^{2-} + 2CO_2 \quad (17)$$

Figure 4

On the other hand, the effluent of municipal wastewater plant from Bogotá-Colombia (EWWTP, Table SM5) doped with LOS (at 11.25 µmol/L, an amount lower than previously used, this to obtain a better approximation to actual concentrations in wastewater) was treated by PEF (Fig. 4B). It was found that the process led to a high degradation of LOS (64% after 120 min of treatment) in such complex matrix. Although the process was efficient for the antihypertensive removal in the EWWTP, its degradation was slower than in distilled water (even when the initial concentration of

LOS was lower). A revision of the EWWTP composition shows that this water has a considerable content of other organic matter (see its COD and TOC values) and ionic substances (as indicated by alkalinity and conductivity) that compete with LOS by the degrading agents as radicals (Salazar et al., 2016). Also, the turbidity and solids in the sample can affect the light action. Moreover, the pH of EWWTP was near neutral (7.65), which decreases the availability of photo-active iron forms as above explained (Eq. 15). Hence, these matrix aspects eliminate the pollutant in the complex matrix slower than in the distilled water.

Conclusions

The treatment of sartan-type antihypertensives by PEF (at mild conditions of current, light, and iron concentration) effectively degraded them in both distilled water and effluent of the wastewater treatment plant. Due to the higher production of oxidizing species (as hydroxyl radical and sulfate radical), the PEF process was more efficient than anodic oxidation or electro-peroxidation to eliminate both LOS and VAL. The structural differences between LOS and VAL determined their interaction with the degrading agents generated in PEF. Indeed, LOS exhibits a higher reactivity toward the species, such as HO•, which is justified by both the faster degradation (a higher k value) and higher atomic charges than VAL. Besides, the generated radicals reacted with the biphenyl-tetrazole rings, imidazole, and alcohol moieties on LOS. Meanwhile, VAL experimented modification on the carboxyl and pentanamide moieties, plus hydroxylations on its biphenyl-tetrazole nucleus. Such modifications on both pollutants agreed well with the reactive sites indicated by the theoretical calculations, revealing the high utility of atomic charge analyses for rationalizing the primary transformations

induced by PEF. This electrochemical process-induced partial mineralization of the two target pollutants (between 33 and 38% after 5 h of treatment) indicates that the compounds coming from the primary products are more recalcitrant to the action of PEF. Additionally, the treatment of LOS at pH around 5 was improved by the presence of oxalic acid. Thanks to this compound, it is avoided the precipitation of iron (III) as ferric oxyhydroxides, and the photo-regeneration of iron (II) is favored. Finally, the process led to a high degradation of LOS in the municipal wastewater treatment plant; however, such degradation was slower than in distilled water because of the interfering effects of the matrix components. The good results about degradation in the effluent and oxalic acid's presence indicate the high potentiality of PEF application to degrade sartan-type antihypertensives in complex matrices containing both organic and inorganic matter.

Acknowledgments

The authors from Universidad Antonio Nariño thank MINCIENCIAS COLOMBIA (formerly known as COLCIENCIAS) for funding through project No. 123384467057 (contract 818-2019 - Call 844-2019). The authors from GIRAB thank Universidad de Antioquia UdeA for the support provided to their research group through “Programa de Sostenibilidad” and the financing from MINCIENCIAS COLOMBIA (before named COLCIENCIAS) through the project No. 111577757323 (Convocatoria 777 de 2017). Authors from IUPA (UJI) acknowledge the financial support of Ministerio de Ciencia, Innovación y Universidades, Spain (Ref RTI 2018-097417-B-I00) and Generalitat Valenciana (Research Group of Excellence, Prometeo 2019/040). E.A. Serna-Galvis

436 thanks the doctoral scholarship provided by MINCIENCIAS COLOMBIA (before named
437 COLCIENCIAS) from July 2015 to June 2019 through Convocatoria 647 de 2014.

438

439 **References**

440 Antonin, V.S., Santos, M.C., Garcia-Segura, S., Brillas, E., 2015. Electrochemical
441 incineration of the antibiotic ciprofloxacin in sulfate medium and synthetic urine
442 matrix. Water Res. 83, 31–41. https://doi.org/10.1016/j.watres.2015.05.066

443 Berkner, S., Thierbach, C., 2014. Biodegradability and transformation of human
444 pharmaceutical active ingredients in environmentally relevant test systems.
445 Environ. Sci. Pollut. Res. 21, 9461–9467. https://doi.org/10.1007/s11356-013-
446 1868-6

447 Billany, M.R., Khatib, K., Gordon, M., Sugden, J.K., 1996. Alcohols and ethanolamines
448 as hydroxyl radical scavengers. Int. J. Pharm. 137, 143–147.
449 https://doi.org/10.1016/0378-5173(96)04246-9

450 Bonfilio, R., Favoretto, L.B., Pereira, G.R., Azevedo, R.D.C.P., Araújo, M.B. de, 2010.
451 Comparative study of analytical methods by direct and first-derivative UV
452 spectrophotometry for evaluation of losartan potassium in capsules. Brazilian J.
453 Pharm. Sci. 46, 147–155. https://doi.org/10.1590/S1984-82502010000100017

454 Botero-Coy, A.M., Martínez-Pachón, D., Boix, C., Rincón, R.J., Castillo, N., Arias-
455 Marín, L.P., Manrique-Losada, L., Torres-Palma, R.A., Moncayo-Lasso, A.,
456 Hernández, F., 2018. 'An investigation into the occurrence and removal of
457 pharmaceuticals in Colombian wastewater.' Sci. Total Environ. 642, 842–853.

458 https://doi.org/10.1016/j.scitotenv.2018.06.088

459 Cheng, Q., Gu, J., Compaan, K.R., Schaefer, H.F., 2010. Hydroxyl radical reactions
460 with adenine: Reactant complexes, transition states, and product complexes.
461 Chem. - A Eur. J. 16, 11848–11858. https://doi.org/10.1002/chem.201001236

462 ClinClac, 2018. Valsartan-number of prescriptions over time (2007-2017) [WWW
463 Document]. Clincalc.com. URL https://clincalc.com/DrugStats/Drugs/Valsartan
464 (accessed 7.4.20).

465 Dao, K.C., Yang, C.-C., Chen, K.-F., Tsai, Y.-P., 2020. Recent Trends in Removal
466 Pharmaceuticals and Personal Care Products by Electrochemical Oxidation and
467 Combined Systems. Water 12, 1043. https://doi.org/10.3390/w12041043

468 Davis, J., Baygents, J.C., Farrell, J., 2014. Understanding Persulfate Production at
469 Boron Doped Diamond Film Anodes. Electrochim. Acta 150, 68–74.
470 https://doi.org/https://doi.org/10.1016/j.electacta.2014.10.104

471 Feng, L., Serna-Galvis, E.A., Oturan, N., Giannakis, S., Torres-Palma, R.A., Oturan,
472 M.A., 2019. Evaluation of process influencing factors, degradation products,
473 toxicity evolution and matrix-related effects during electro-Fenton removal of
474 piroxicam from waters. J. Environ. Chem. Eng. 7, 103400.
475 https://doi.org/10.1016/j.jece.2019.103400

476 Gurkan, Y.Y., Turkten, N., Hatipoglu, A., Cinar, Z., 2012. Photocatalytic degradation of
477 cefazolin over N-doped TiO2 under UV and sunlight irradiation: Prediction of the
478 reaction paths via conceptual DFT. Chem. Eng. J. 184, 113–124.
479 https://doi.org/10.1016/j.cej.2012.01.011

Gurke, R., Rößler, M., Marx, C., Diamond, S., Schubert, S., Oertel, R., Fauler, J., 2015. Science of the Total Environment Occurrence and removal of frequently prescribed pharmaceuticals and corresponding metabolites in wastewater of a sewage treatment plant. Sci. Total Environ. 532, 762–770. https://doi.org/10.1016/j.scitotenv.2015.06.067

He, X., Mezyk, S.P., Michael, I., Fatta-Kassinos, D., Dionysiou, D.D., 2014. Degradation kinetics and mechanism of β-lactam antibiotics by the activation of H2O2 and Na2S2O8 under UV-254nm irradiation. J. Hazard. Mater. 279, 375–383. https://doi.org/10.1016/j.jhazmat.2014.07.008

Ionescu, C.M., Sehnal, D., Falginella, F.L., Pant, P., Pravda, L., Bouchal, T., Svobodová Vařeková, R., Geidl, S., Koča, J., 2015. AtomicChargeCalculator: Interactive web-based calculation of atomic charges in large biomolecular complexes and drug-like molecules. J. Cheminform. 7, 1–13. https://doi.org/10.1186/s13321-015-0099-x

Israili, Z.H., 2000. Clinical pharmacokinetics of angiotensin II (AT 1) receptor blockers in hypertension. J Hum Hypertens Suppl. 1, S73-87.

Kaur, B., Dulova, N., 2020. UV-assisted chemical oxidation of antihypertensive losartan in water. J. Environ. Manage. 261, 110170. https://doi.org/10.1016/j.jenvman.2020.110170

Khan, S., He, X., Khan, J.A., Khan, H.M., Boccelli, D.L., Dionysiou, D.D., 2017. Kinetics and mechanism of sulfate radical- and hydroxyl radical-induced degradation of highly chlorinated pesticide lindane in UV/peroxymonosulfate system. Chem. Eng.

J. 318, 135–142. https://doi.org/10.1016/j.cej.2016.05.150

Liu, Y., He, X., Fu, Y., Dionysiou, D.D., 2016. Kinetics and mechanism investigation on the destruction of oxytetracycline by UV-254 nm activation of persulfate. J. Hazard. Mater. 305, 229–239. https://doi.org/10.1016/j.jhazmat.2015.11.043

Llano, J., Eriksson, L.A., 1999. Mechanism of Hydroxyl Radical Addition to Imidazole and Subsequent Water Elimination. J. Phys. Chem. 103, 5598. https://doi.org/10.1021/jp9902957

Martínez-Pachón, D., Espinosa-Barrera, P., Rincón-Ortíz, J., Moncayo-Lasso, A., 2019. Advanced oxidation of antihypertensives losartan and valsartan by photo-electro-Fenton at near-neutral pH using natural organic acids and a dimensional stable anode-gas diffusion electrode (DSA-GDE) system under light emission diode (LED) lighting. Environ. Sci. Pollut. Res. 26, 4426–4437. https://doi.org/10.1007/s11356-018-2645-3

Martínez-Pachón, D., Ibáñez, M., Hernández, F., Torres-Palma, R.A., Moncayo-Lasso, A., 2018. Photo-electro-Fenton process applied to the degradation of valsartan: Effect of parameters, identification of degradation routes and mineralization in combination with a biological system. J. Environ. Chem. Eng. 6, 7302–7311. https://doi.org/10.1016/j.jece.2018.11.015

Mikulic, M., 2020. Number of losartan potassium prescriptions in the U.S. from 2004 to 2017 [WWW Document]. Stat. GmbH. URL https://www.statista.com/statistics/781681/losartan-potassium-prescriptions-number-in-the-us/ (accessed 4.29.20).

524 Moreira, F.C.F.C., Boaventura, R.A.R.R., Brillas, E., Vilar, V.J.P.P., 2017.
525 Electrochemical advanced oxidation processes: A review on their application to
526 synthetic and real wastewaters. Appl. Catal. B Environ. 202, 217–261.
527 https://doi.org/10.1016/j.apcatb.2016.08.037

528 Nödler, K., Hillebrand, O., Idzik, K., Strathmann, M., Schiperski, F., Zirlewagen, J.,
529 Licha, T., 2013. Occurrence and fate of the angiotensin II receptor antagonist
530 transformation product valsartan acid in the water cycle - A comparative study with
531 selected β-blockers and the persistent anthropogenic wastewater indicators
532 carbamazepine and acesulfame. Water Res. 47, 6650–6659.
533 https://doi.org/10.1016/j.watres.2013.08.034

534 Pignatello, J.J., Oliveros, E., Mackay, A., 2006. Advanced Oxidation Processes for
535 Organic Contaminant Destruction Based on the Fenton Reaction and Related
536 Chemistry. Crit. Rev. Environ. Sci. Technol. 36, 1–84.
537 https://doi.org/10.1080/10643380500326564

538 Rueffer, M., Bejan, D., Bunce, N.J., 2011. Graphite: An active or an inactive anode?
539 Electrochim. Acta 56, 2246–2253. https://doi.org/10.1016/j.electacta.2010.11.071

540 Salazar, C., Contreras, N., Mansilla, H.D., Yáñez, J., Salazar, R., 2016.
541 Electrochemical degradation of the antihypertensive losartan in aqueous medium
542 by electro-oxidation with boron-doped diamond electrode. J. Hazard. Mater. 319,
543 84–92. https://doi.org/10.1016/j.jhazmat.2016.04.009

544 Sehnal, D., 2020. AtomicChargeCalculator [WWW Document]. WebChemistry. URL
545 https://webchem.ncbr.muni.cz/Platform/ChargeCalculator (accessed 4.27.20).

546 Serna-Galvis, E.A., Ferraro, F., Silva-Agredo, J., Torres-Palma, R.A., 2017.
547 Degradation of highly consumed fluoroquinolones, penicillins and cephalosporins
548 in distilled water and simulated hospital wastewater by UV254 and
549 UV254/persulfate processes. Water Res. 122, 128–138.
550 https://doi.org/10.1016/j.watres.2017.05.065

551 Serna-Galvis, E.A., Isaza-Pineda, L., Moncayo-Lasso, A., Hernández, F., Ibáñez, M.,
552 Torres-Palma, R.A., 2019. Comparative degradation of two highly consumed
553 antihypertensives in water by sonochemical process. Determination of the
554 reaction zone, primary degradation products and theoretical calculations on the
555 oxidative process. Ultrason. Sonochem. 58, 104635.
556 https://doi.org/10.1016/j.ultsonch.2019.104635

557 Serna-Galvis, E.A., Silva-Agredo, J., Giraldo-Aguirre, A.L., Torres-Palma, R.A., 2015.
558 Sonochemical degradation of the pharmaceutical fluoxetine: Effect of parameters,
559 organic and inorganic additives and combination with a biological system. Sci.
560 Total Environ. 524–525, 354–360. https://doi.org/10.1016/j.scitotenv.2015.04.053

561 Singh, S., Yadav, A.K., Gautam, H., 2011. Simultaneous Estimation of Valsartan and
562 Hydrochlorothiazide in Tablets By Rp-Hplc Method. Bull. Pharm. Res. 170–174.

563 Sirés, I., Brillas, E., 2012. Remediation of water pollution caused by pharmaceutical
564 residues based on electrochemical separation and degradation technologies : A
565 review. Environ. Int. 40, 212–229. https://doi.org/10.1016/j.envint.2011.07.012

566 Sirés, I., Brillas, E., Oturan, M.A., Rodrigo, M.A., Panizza, M., 2014. Electrochemical
567 advanced oxidation processes: today and tomorrow. A review. Environ. Sci. Pollut.

Res. 21, 8336–8367. https://doi.org/10.1007/s11356-014-2783-1

Skoumal, M., Rodríguez, R.M., Cabot, P.L., Centellas, F., Garrido, J.A., Arias, C., Brillas, E., 2009. Electro-Fenton, UVA photoelectro-Fenton and solar photoelectro-Fenton degradation of the drug ibuprofen in acid aqueous medium using platinum and boron-doped diamond anodes. Electrochim. Acta 54, 2077–2085. https://doi.org/10.1016/j.electacta.2008.07.014

Steffen, L.K., Glass, R.S., Sabahi, M., Wilson, G.S., Schoeneich, C., Mahling, S., Asmus, K.D., 1991. Hydroxyl radical induced decarboxylation of amino acids. Decarboxylation vs bond formation in radical intermediates. J. Am. Chem. Soc. 113, 2141–2145. https://doi.org/10.1021/ja00006a035

Transparency Market Research, 2020. Oxalic Acid Market [WWW Document]. Oxalic Acid Mark. - Glob. Ind. Anal. Size, Share, Growth, Trends, Forecast 2019 - 2027. URL https://www.transparencymarketresearch.com/oxalic-acid-market.html (accessed 4.1.20).

Yang, Y., Jiang, J., Lu, X., Ma, J., Liu, Y., 2015. Production of Sulfate Radical and Hydroxyl Radical by Reaction of Ozone with Peroxymonosulfate: A Novel Advanced Oxidation Process. Environ. Sci. Technol. 49, 7330–7339. https://doi.org/10.1021/es506362e

588

589 **Figure Captions**

590 A

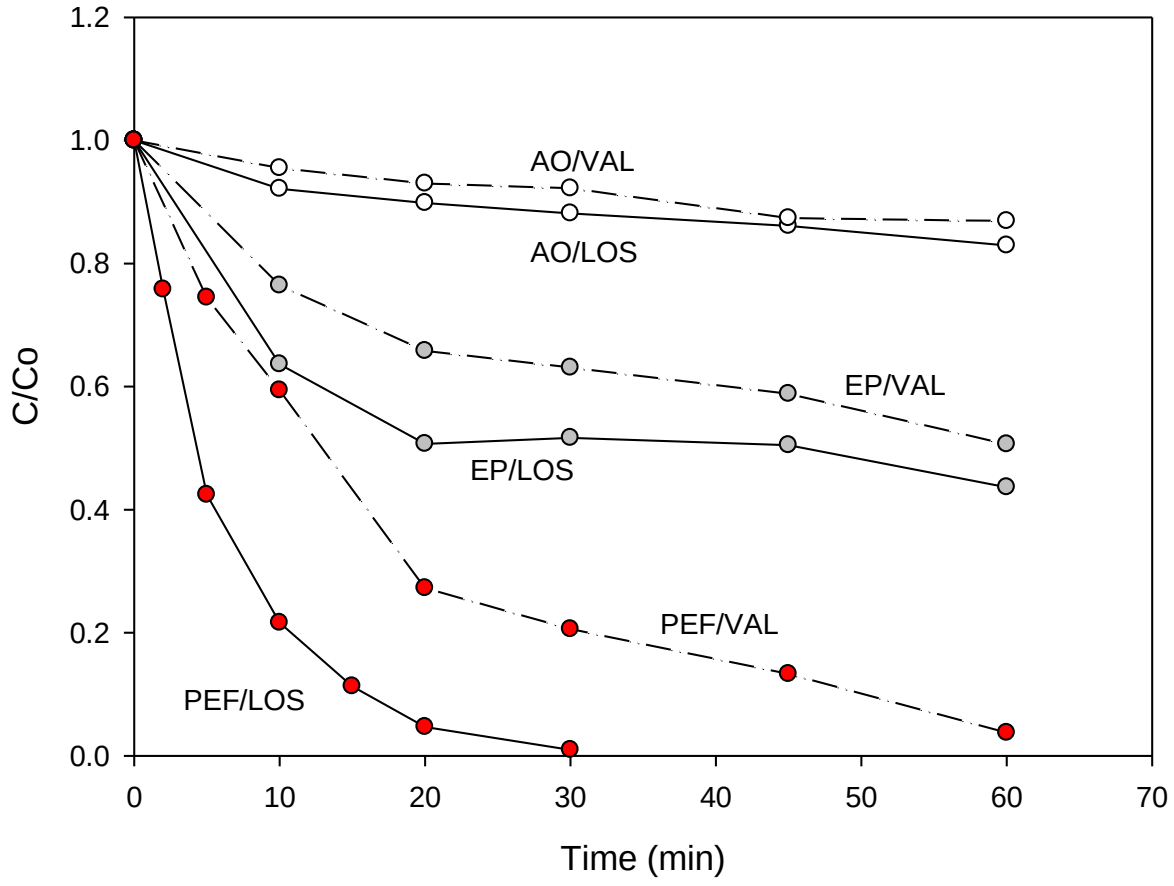

591

592

593

594

595

596

597

598 B

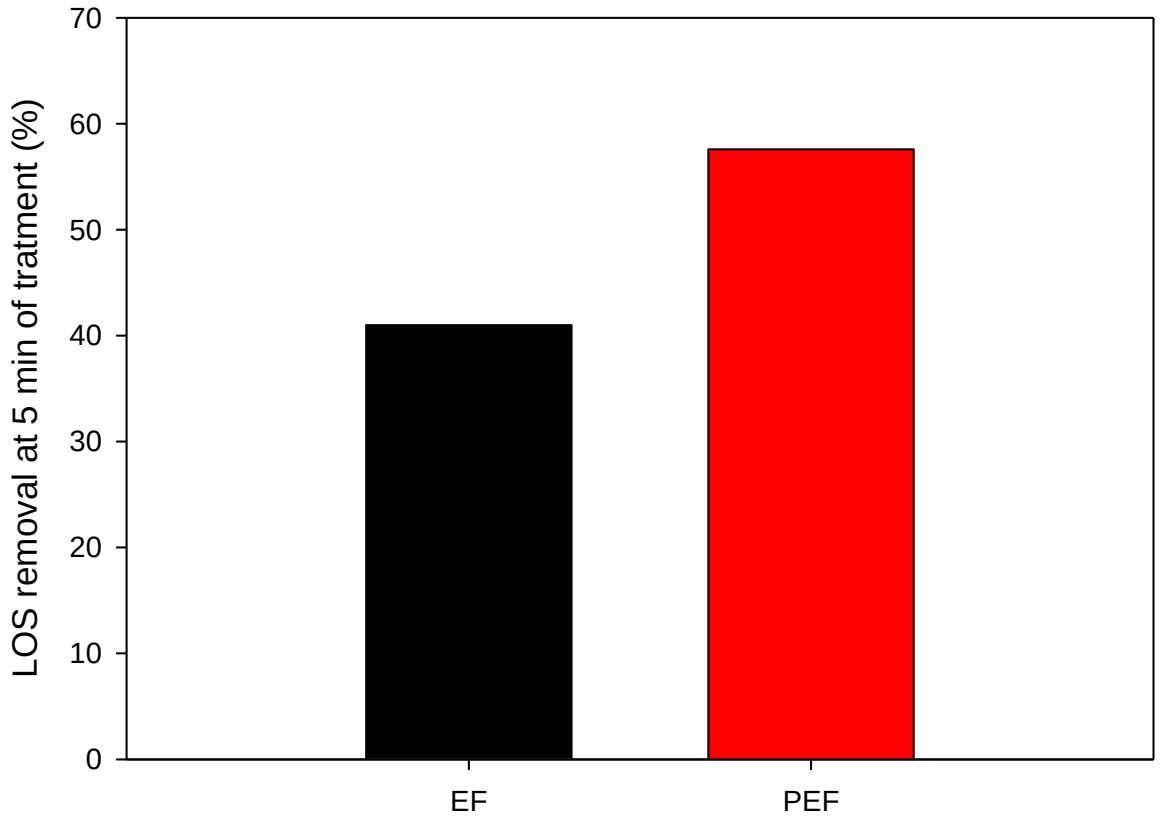

599

600

601

602

603

604

605

606

C

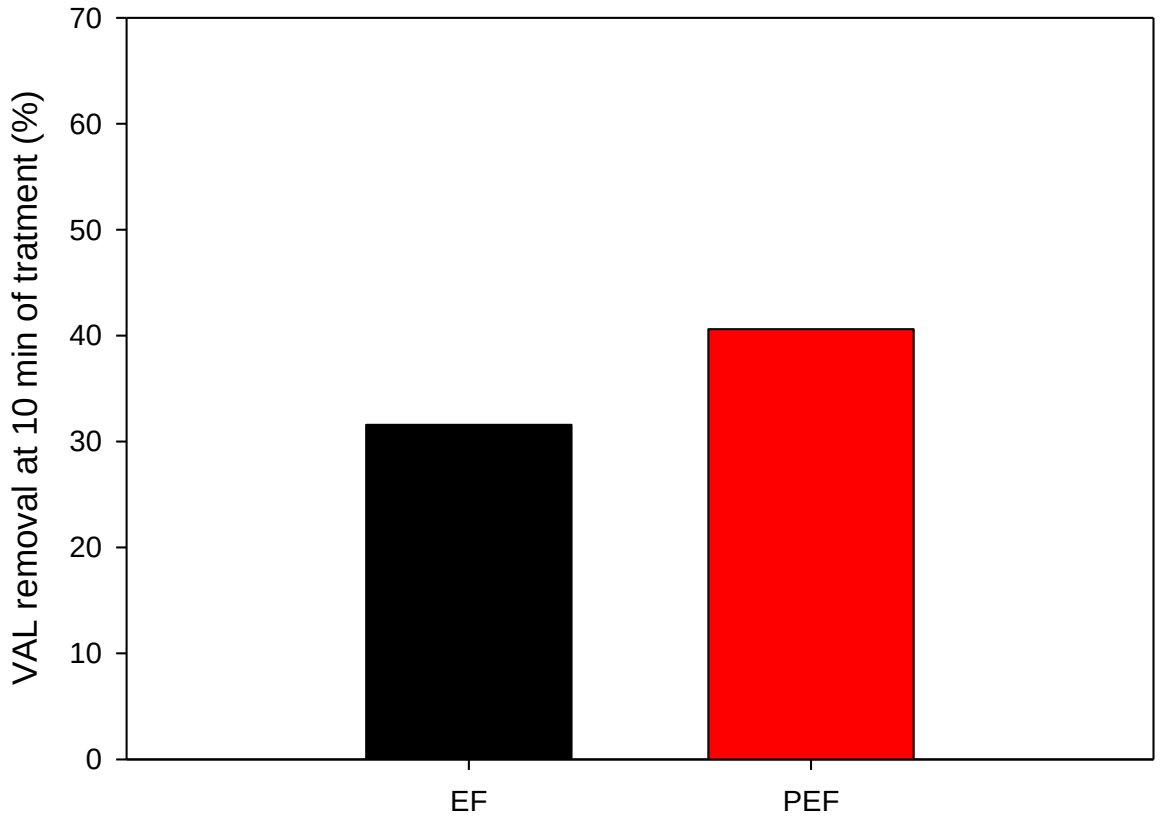

Figure 1. LOS and VAL degradation by the electrochemical systems **A.** Comparison among anodic oxidation (AO: BDD/SS), electro-peroxidation (EP: graphite/GDE) and photo-electro-Fenton (PEF: BDD/GDE/UVA) system. **B and C**: Comparison among electro-Fenton (EF: BDD/GDE) and photo-electro-Fenton (PEF: BDD/GDE/UVA) systems. Experimental conditions: [antihypertensive]: 45 µmol/L, V: 200 mL, pH initial: 3.0, [Na_2SO_4]: 0.05 mol/L

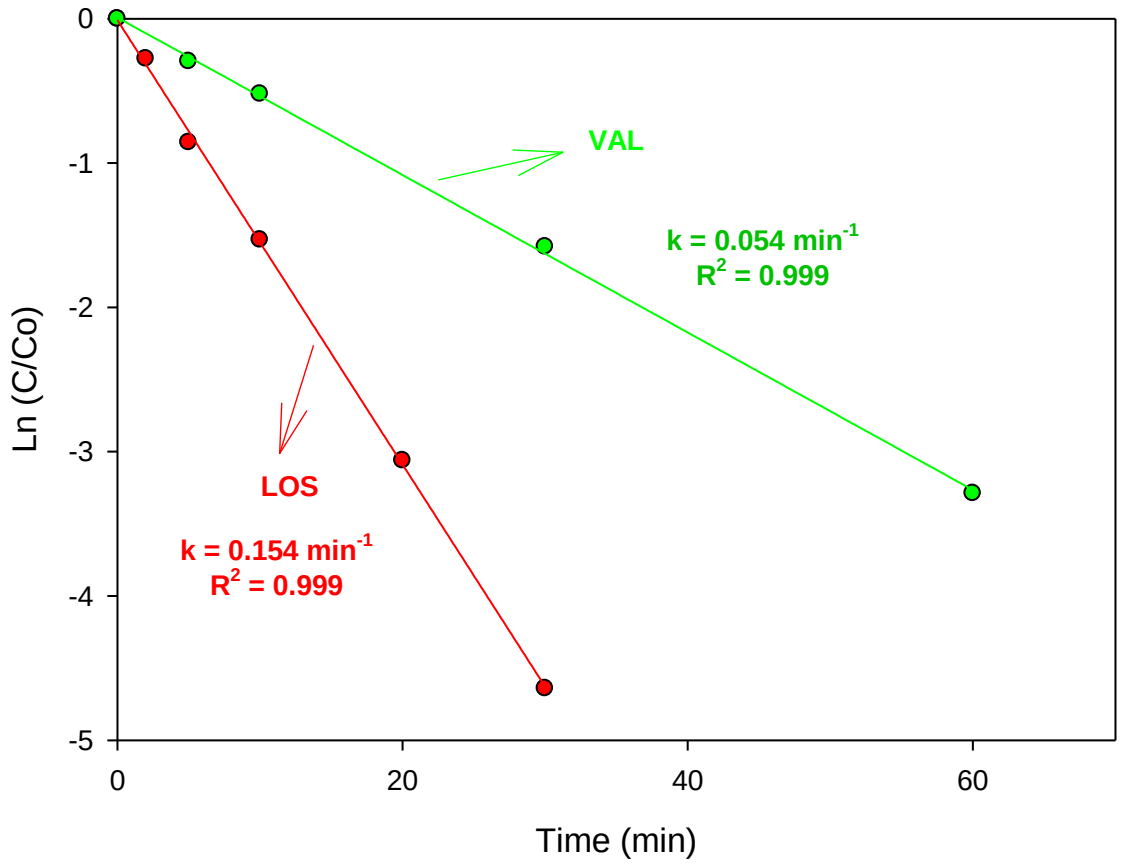

Figure 2. Determination of pseudo-first order kinetics constants (k) for losartan (LOS) and valsartan (VAL) degradation by PEF. Experimental conditions: [antihypertensive]: 45 µmol/L, V: 200 mL, pH initial: 3.0, $[Fe^{2+}]$: 36 µmol/L, Light UV-A (368 nm), $[Na_2SO_4]$: 0.05 mol/L

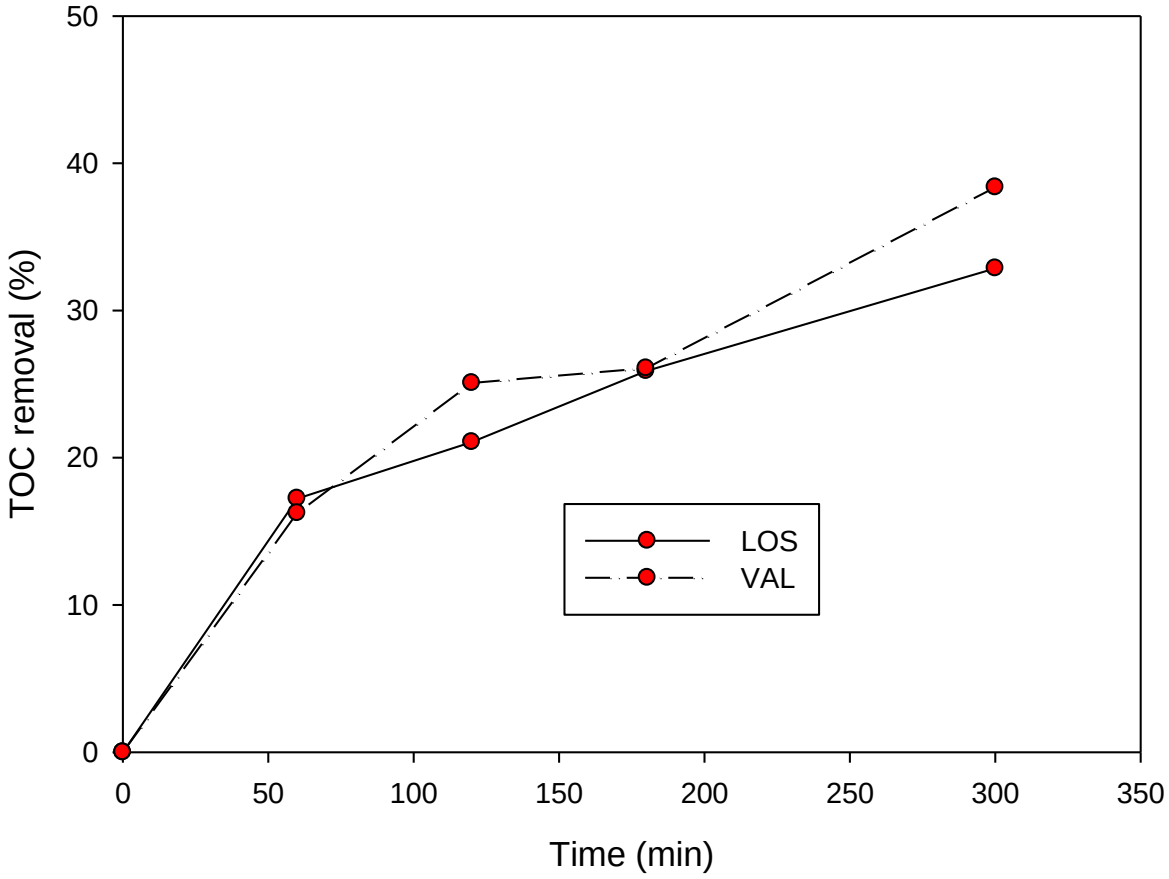

627

628 **Figure 3.** TOC evolution for LOS degradation by PEF. TOC initial: 12.1 mg C/L

629 Experimental conditions: [LOS]: 45 µmol/L, V: 200 mL, pH initial: 3.0, [Fe^{2+}]: 36

630 µmol/L, Light UV-A (368 nm), [Na_2SO_4]: 0.05 mol/L

631

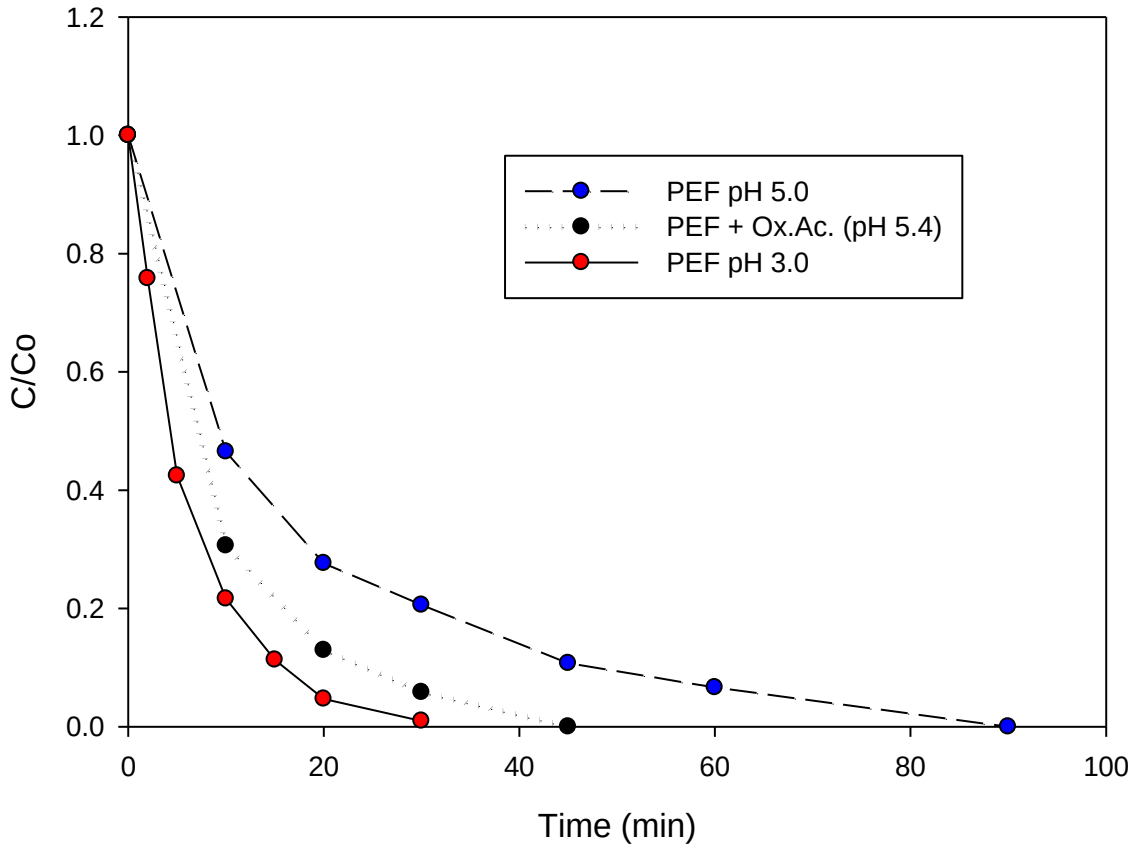
1.2
1.0
0.8
0.6
0.4
0.2
0.0
C/Co
0
20
40
60
80
100
Time (min)
PEF pH 5.0
PEF + Ox.Ac. (pH 5.4)
PEF pH 3.0

632

633

634 B

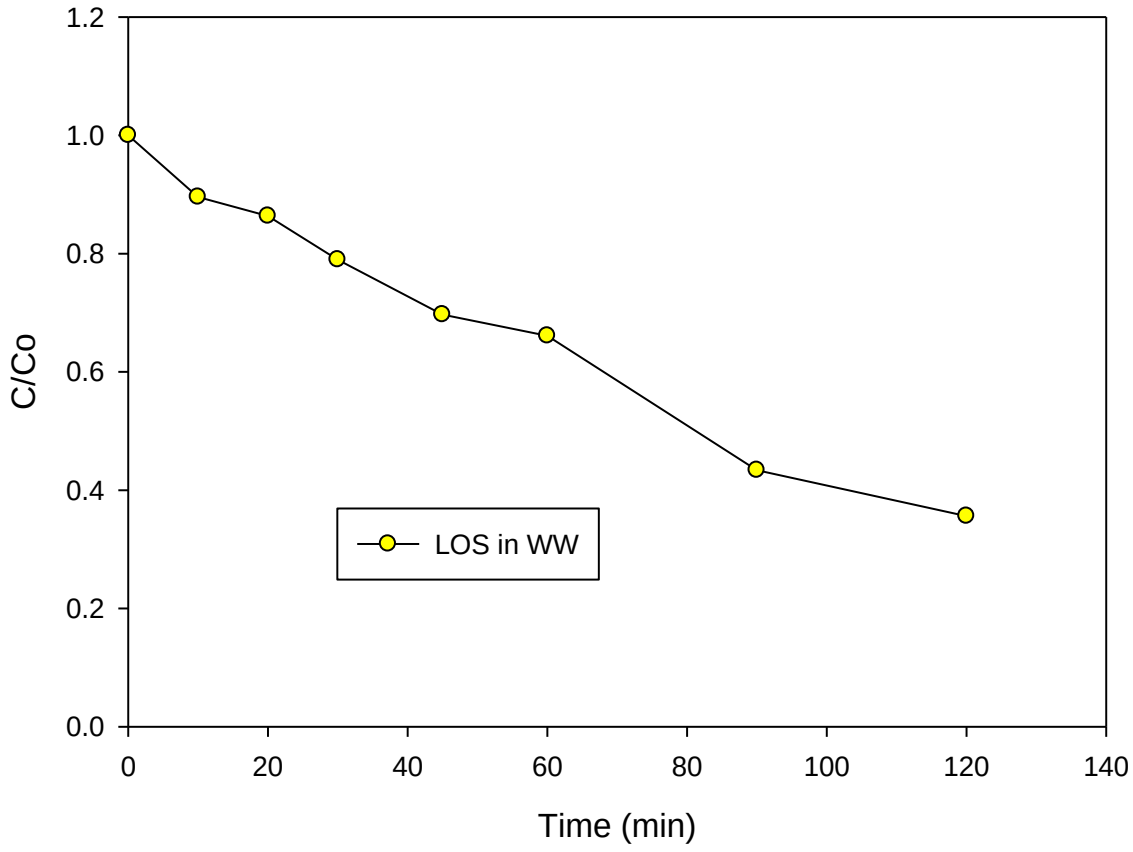

Figure 4. A Degradation of LOS in the presence of oxalic acid by PEF (BDD/GDE/UVA/Na_2SO_4) at pH 3.0 and pH ~5.0 in absence of oxalic acid, plus at pH 5.0 in presence of oxalic acid (Ox. Ac, 40 µmol/L). Experimental conditions: [LOS]: 45 µmol/L, V: 200 mL, [Fe^{2+}]: 36 µmol/L, [Oxalic acid]: 40 µmol/L, [Na_2SO_4]: 0.05 mol/L. **B.** LOS (11.25 µmol/L) degradation in real complex water.